OPEN-CIRCUIT VOLTAGE IMPROVEMENTS IN LOW-RESISTIVITY SOLAR CELLS

Michael P. Godlewski, Thomas M. Klucher, George A. Mazaris
and Victor G. Weizer
National Aeronautics and Space Administration
Lewis Research Center

The Lewis Research Center has been engaged in an attempt to identify the mechanisms limiting the open-circuit voltage in 0.1-ohm-cm solar cells. In the course of this work it was found that a rather complicated multistep diffusion process could produce cells with significantly improved voltages. Concurrent with the Lewis effort, several other laboratories have been pursuing alternative approaches under various NASA contracts. The best Lewis results to date and the best results from other laboratories are compared in figure 1. Together with the Lewis results, the figure shows the air-mass-zero (AMO) open-circuit voltage as a function of the short-circuit current for the University of Florida's charged-oxide, high-low emitter cell and for the Spire Corporation's ion-implanted emitter cells and published results for the University of New South Wales' metal-insulator-seminconductor (MIS) cell (ref. 1). To compare the voltage capabilities of these cells, independent of their absorption and collection efficiencies, we must compare them on the basis of their saturation currents or, equivalently, compare their voltage outputs at a constant current-density level. If we arbitrarily choose 25 mA/cm^2 or, as plotted in figure 1, 100 mA/4 cm^2 as the reference current density and assume ideal diode characteristics, we see that the highest voltage (648 mV) is obtained from the Florida cell. The Lewis cell and the Spire cell yield about 637 millivolts, and the New South Wales cell about 632 millivolts. The open-circuit voltage is defined throughout this paper as the voltage obtained at a current density of 25 mA/cm .

The Lewis multistep fabrication schedule is described in figure 2, along with a list of processing conditions that have resulted from a partial optimization effort. The schedule consists of three steps, all of which have been found to be necessary. The first step is a relatively deep diffusion. This primary diffusion is followed by an acid-etch removal of the emitter surface such that the final sheet resistance is in the 10- to 12-ohm/ range. The etching step is then followed by a short, low-temperature secondary diffusion. Final junction depths ranged from 1 to 4 micrometers.

As stated, the schedule has not been completely optimized. Consider, for example, the time of the primary diffusion. As shown in figure 3, we have found a direct correlation between the primary diffusion time and the open-circuit voltage. As can be seen, the highest voltage was obtained for the longest diffusion time (i.e., 637 mV for a 65-hr diffusion).

As the diffusion time is lengthened, cell fabrication becomes increasingly cumbersome. It was decided, therefore, for experimental expediency, to investigate the mechanisms associated with the increase in diffusion time that lead

to improved voltages. The identification of these mechanisms should permit us to achieve the increased voltages in more conventional structures.

The first step in the investigation was to determine which region of the cell was responsible for voltage control (i.e., base, emitter, or depletion region). Since the cells fabricated by the multistep technique exhibit ideal diode characteristics, depletion region effects were ruled out.

To determine the degree of control exercised by the base and emitter components of the saturation current, several experiments were performed. In figure 4 the open-circuit voltage is plotted as a function of the base diffusion length as measured by the X-ray technique for cells receiving a 4-hour, 950° C primary diffusion. The other fabrication conditions for these cells are as indicated in figure 3. Superimposed on the data in figure 4 are those calculated curves that have been fit to the data at the point indicated. The upper curve is what would be expected if the base component of the saturation current were only 10 percent of the total saturation current as calculated at the fit point. Also shown are what would be expected for 40 and 100 percent base control. The closest fit occurs when we assume complete base control.

A similar plot for cells diffused at 950° C for 41 hours is given in figure 5. The voltages in this plot are generally higher than those in figure 4, an indication of reduction of the base saturation current with increasing diffusion time. A similar set of calculated curves on this plot indicate base control, although there is now some evidence of emitter influence. Best agreement with the experimental data is obtained for the case where, at the fit point, the base contributes 80 percent of the device saturation current and the emitter 20 percent.

These two plots correlate with the results of the spectral response measurements made both with 0.5-micrometer-wavelength light, which is absorbed completely in the emitter, and 0.9-micrometer-wavelength light, which is absorbed mostly in the base. Figure 6 shows the relationship between the open-circuit voltage and the monochromatic 0.5- and 0.9-micrometer spectral responses for cells fabricated with 4-hour, 950° C primary diffusions. The parameters that affect the current output from a given region of the cell (i.e., base or emitter) should also affect the value of the saturation current from that region. If, therefore, the base component of the saturation current were controlling the voltage, we would expect a positive correlation between the base current (0.9-μm response) and the open-circuit voltage. That figure 6 shows such a correlation is further evidence that the base is voltage controlling in these cells.

These arguments apply in a similar fashion to the emitter region. The lack of correlation between the voltage and the emitter current (0.5-μm response) is consistent with the notion of base control.

These current-voltage arguments, although convincing, are not absolutely conclusive. It is conceivable that some emitter current - such as the diffusivity, which does not affect the emitter current - is actually controlling the cell voltage. However, to be consistent with the data, this emitter parameter would have to be fortuitously correlated with the base current - a situation which, although possible, is very unlikely. These data, therefore, along with

those presented in figures 4 and 5, strongly suggest that the open-circuit voltage of the Lewis multistep diffusion cell is controlled by the base component of the cell saturation current.

Similar spectral response - voltage plots for a limited sampling of Florida high-low emitter cells and Spire ion-implanted cells are shown in figure 7. The red response-voltage correlation for the Spire cells indicated probable base control. The data for the Florida cells, on the other hand, are not very conclusive. There does not appear to be the same correlation with red response as for the other cells, a possible indication of emitter control. The results of 1-MeV-electron irradiation experiments performed at Lewis (ref. 2) on these three cell types support the above conclusions (i.e., base control for the Lewis and Spire cells and emitter control for the Florida cells).

The preceding data suggest strongly that the open-circuit voltage in the Lewis diffused cells is controlled by the base component of the saturation current. It remains now to identify which parameter in that component is being influenced by the primary diffusion time in such a way as to yield increased voltages as the time is lengthened.

Assuming a high recombination velocity at the rear surface of the cell, the base saturation current, I_{OB}, is given by the well-known expression:

$$I_{OB} = \frac{qn_i^2 D}{N_A L} \coth \frac{d}{L} \tag{1}$$

where q is electronic charge, n_i is intrinsic carrier concentration, D is diffusivity, N_A is acceptor impurity concentration, L is diffusion length, and d is base-region width. In an attempt to isolate the voltage-controlling parameter, three cells were selected that had widely different open-circuit voltages but nearly identical base diffusion lengths, thicknesses, and rear surface treatments. The primary diffusion times for these cells were 4, 16, and 41 hours. Again, these cells and all the cells discussed in this paper exhibited ideal, diffusion-controlled current-voltage characteristics. It was reasoned that the voltage differences between these cells must be due to differences in either the boron concentration and/or profile or the base minority carrier diffusivity.

The electrically active boron concentration profiles in these three cells were determined indirectly through a SIMS measurement of their phosphorus profiles. The SIMS data are shown in figure 8, along with other data for these cells. The diffusion lengths in these cells were the same to within a few percent, as were their thicknesses. In the figure the phosphorus concentration is plotted as a function of distance from the junction. The profiles near the depletion region are unexpectedly similar. In fact, they appear to be identical. This anomalous result is due to an unexplained retardation of the phosphorus diffusion front that intensifies as the diffusion time is increased. Although such retardation phenomena have been reported in the literature (ref. 3), the mechanisms involved are still unclear.

The net, or electrically active, boron concentration on the base side of the junction can be obtained by subtracting the measured phosphorus concentration from the prediffusion boron concentration. Since these cells were all fabricated from the same silicon ingot, the calculated postdiffusion net boron concentration profiles must be identical.

We can conclude, therefore, that because the net boron profiles, the base diffusion lengths, the thicknesses, and the rear surface recombination velocities of these cells are identical, the observed voltage differences must be due to differences in the remaining variable (i.e., the base minority carrier mobility). To explain the observed voltage increases, one would have to invoke a reduction in the electron mobility in the base as the diffusion time is increased.

The validity of these conclusions could be tested through a measurement of the base mobility of these three cells. Theoretically this could be done by making independent measurements of the diffusion length and the lifetime and employing the well-known relation

$$L = (D\tau)^{1/2} \tag{2}$$

where L is diffusion length and τ is minority carrier lifetime. Unfortunately, attempts to measure τ in the above cells using a transient open-circuit-voltage decay technique were unsuccessful because of ambiguities in the interpretation of the decay curves. We can, however, present some evidence to attest to the existence of large changes in minority carrier mobility with diffusion time.

The data presented in figure 9 were obtained at Lewis several years ago during a study of shallow-junction, 10-ohm-cm devices. It can be seen that as the diffusion time was increased, the diffusion lengths decreased significantly. However, contrary to what would be expected, as the diffusion lengths decreased, the open-circuit voltages increased. The lifetimes of these cells were measured using an open-circuit voltage decay (OCVD) technique, and the diffusivities calculated using equation (2). The results, shown in figure 9, indicate a large drop in the value of D as the diffusion time was increased from 30 minutes to 2 hours. The decrease in the diffusivity in this case was apparently sufficient to overcome the effects of the decreasing diffusion length and to produce an increase in voltage, even though the diffusion length was severely degraded. These effects are very similar to what has been observed for the present Lewis low-resistivity cells. It appears reasonable, therefore, on the basis of the data presented above, to ascribe the voltage limiting role in the Lewis low-resistivity cells to the electron mobility (diffusivity) in the cell base.

In summary, it appears that for both the Lewis diffused emitter cell and the Spire ion-implanted emitter cell the base component of the saturation current is voltage controlling. The evidence for the University of Florida cells, although not very conclusive, suggests emitter control of the voltage in this device. The data suggest further that the critical voltage-limiting parameter for the Lewis cell is the electron movility in the cell base. The mechanisms involved in the observed mobility changes, however, await further study.

REFERENCES

1. Godfrey, R. B.; and Green, M. A.: 655 mV Open-Circuit Voltage, 17.6% Efficient Silicon MIS Solar Cells. Appl. Phys. Lett. vol. 34, no. 11, June, 1979, pp. 790-793.

2. Weinberg, Irving; Swartz, Clifford K.; and Weizer, Victor G.: Radiation Damage in High-Voltage Silicon Solar Cells. Solar Cell High Efficiency and Radiation Damage - 1979, NASA CP-2097, 1979.

3. Matsumoto, S.; et al.: Effects of Diffusion-Induced Strain and Dislocation on Phosphorus Diffusion into Silicon. J. Electrochem. Soc., vol. 125, no. 11, Nov. 1978, pp. 1840-1845.

COMPARISON OF VOLTAGE IMPROVEMENTS IN 0.1 OHM-CM SILICON CELLS.

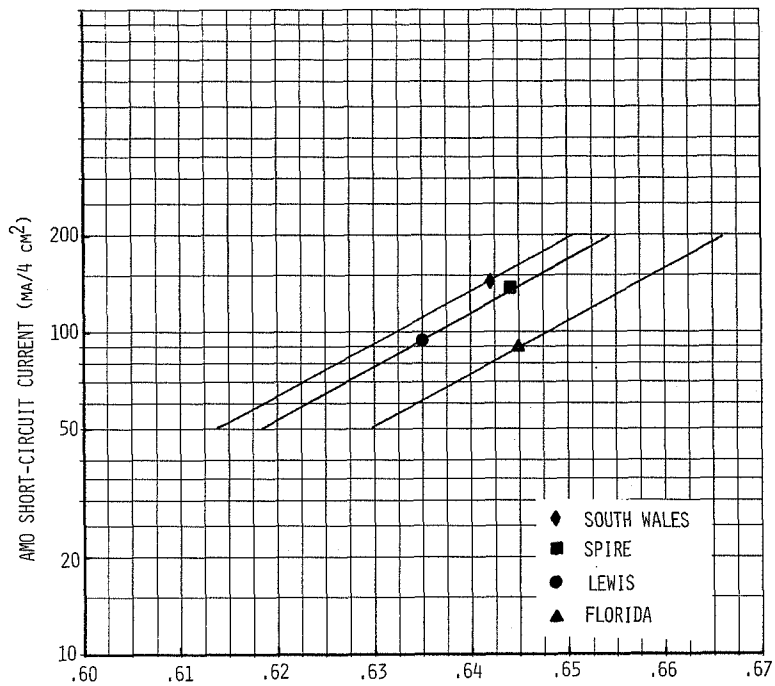

FIGURE 1

LEWIS CELL FABRICATION SCHEDULE

1. PRIMARY DIFFUSION

SURFACE CONCENTRATION	1×10^{20} CM^{-3}
TEMPERATURE	950° C
TIME	$\geqslant$ 65 HRS.

2. EMITTER ETCH

SHEET RESISTANCE	10-12 OHM/□

3. SECONDARY DIFFUSION

SURFACE CONCENTRATION	2×10^{20} CM^{-3}
TEMPERATURE	750° C
TIME	15 MIN.

FIGURE 2

OPEN-CIRCUIT VOLTAGE AS A FUNCTION OF PRIMARY DIFFUSION TIME

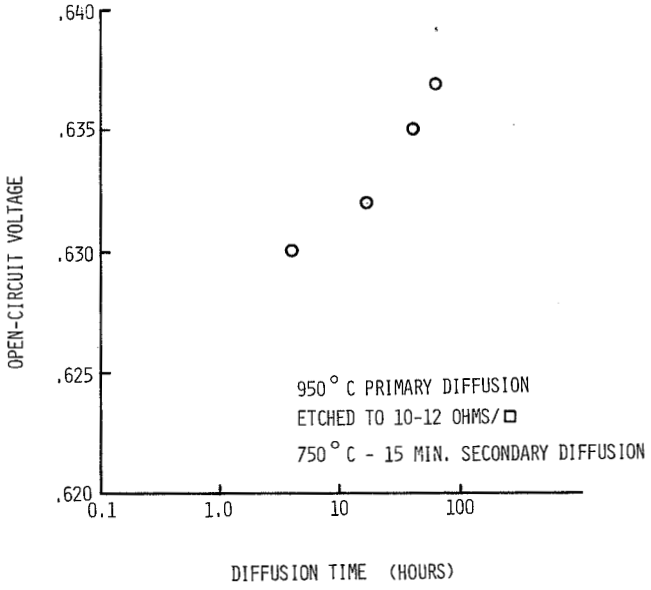

FIGURE 3

INFLUENCE OF BASE DIFFUSION LENGTH ON VOLTAGE

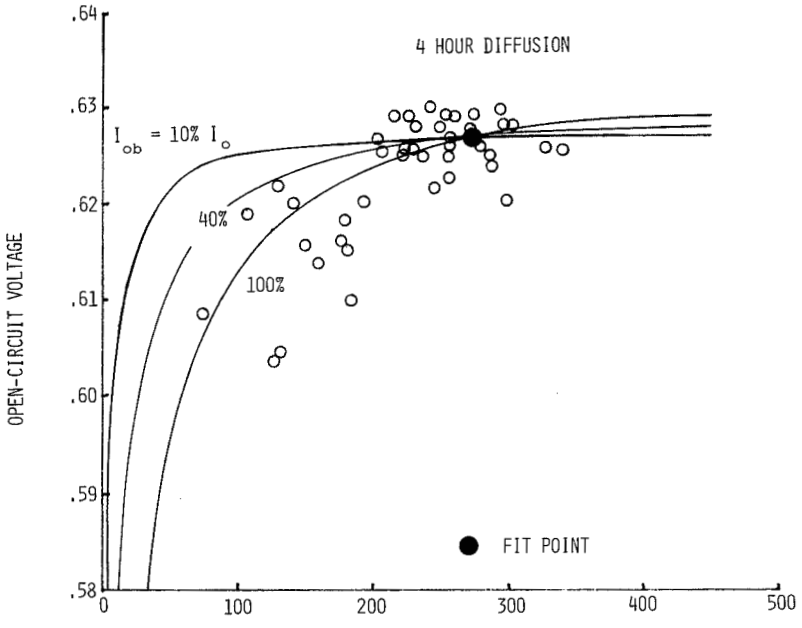

FIGURE 4

INFLUENCE OF BASE DIFFUSION LENGTH ON VOLTAGE

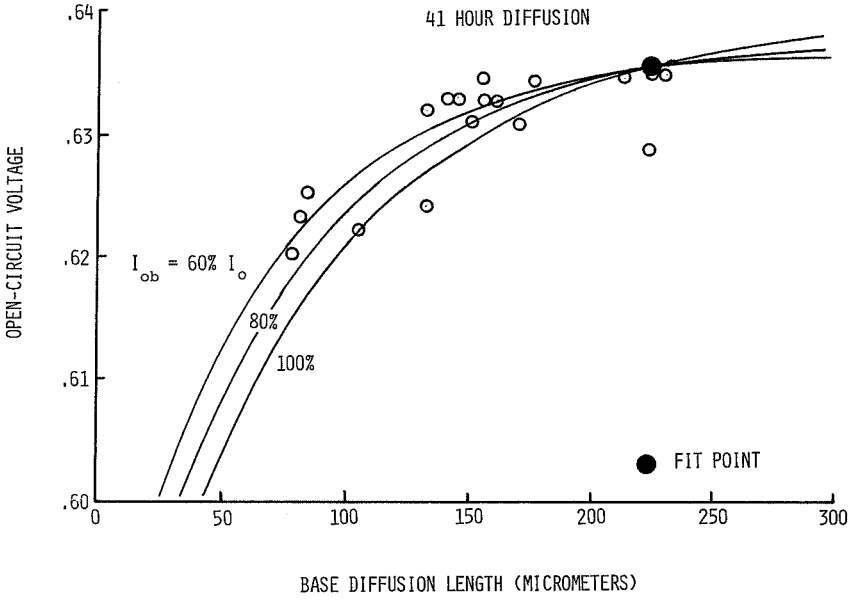

FIGURE 5

CORRELATION BETWEEN VOLTAGE AND CURRENT FOR SELECTED WAVELENGTHS

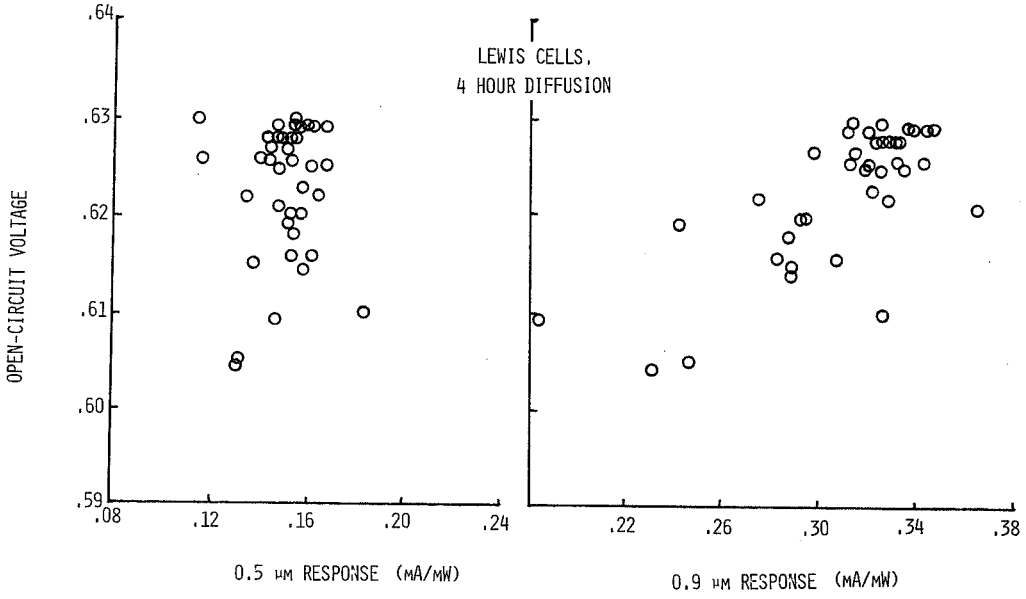

FIGURE 6

CORRELATION BETWEEN VOLTAGE AND CURRENT FOR SELECTED WAVELENGTHS

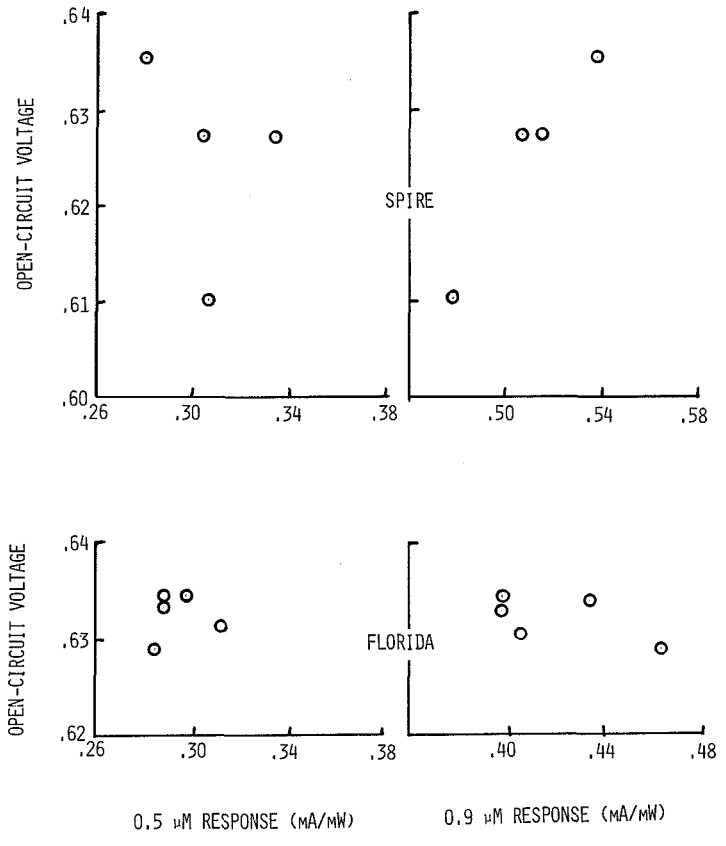

FIGURE 7

EFFECT OF PRIMARY DIFFUSION TIME ON PHOSPHORUS CONCENTRATION PROFILE (SIMS)

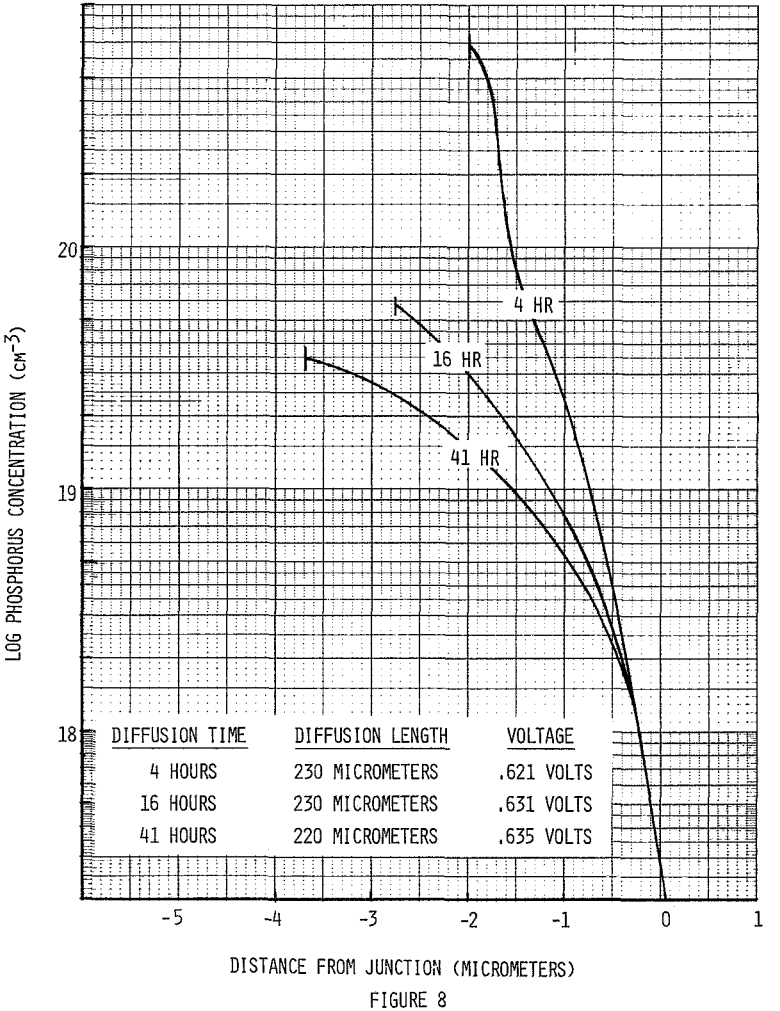

FIGURE 8

EFFECT OF DIFFUSION TIME ON MINORITY CARRIER DIFFUSIVITY

DIFFUSION CONDITIONS	V_{OC}^{25}	$L^{(A)}$	$\tau^{(B)}$	$D(\tau)$
750 - 30 MIN	.523 V	120 μM	2.0 μSEC	72.0 $\frac{CM^2}{SEC}$
750 - 60 MIN	.524 V	70 μM	2.0 μSEC	24.5 "
750 - 120 MIN	.527 V	36 μM	2.3 μSEC	5.6 "

(A) X-RAY TECHNIQUE

(B) OCVD TECHNIQUE

FIGURE 9